Current Biology, Vol. 12, 1611–1616, September 17, 2002, ©2002 Elsevier Science Ltd. All rights reserved. PII S0960-9822(02)01144-2

Drosophila atonal Fully Rescues the Phenotype of *Math1* Null Mice: New Functions Evolve in New Cellular Contexts

Vincent Y. Wang,[1,7] Bassem A. Hassan,[3,5,7] Hugo J. Bellen,[1,2,3] and Huda Y. Zoghbi[1,2,3,4,6]
[1]Program in Developmental Biology
[2]Howard Hughes Medical Institute
[3]Department of Molecular and Human Genetics
[4]Department of Pediatrics
Baylor College of Medicine
Houston, Texas
[5]Department of Human Genetics
Flanders Interuniversity Institute of Biotechnology
Katholieke Universiteit Leuven
Leuven
Belgium

Summary

Many genes share sequence similarity between species, but their properties often change significantly during evolution. For example, the *Drosophila* genes *engrailed* and *orthodenticle* [1, 2] and the onychophoran gene *Ultrabithorax* [3] only partially substitute for their mouse or *Drosophila* homologs. We have been analyzing the relationship between *atonal* (*ato*) in the fruit fly and its mouse homolog, *Math1*. In flies, *ato* acts as a proneural gene that governs the development of chordotonal organs (CHOs), which serve as stretch receptors in the body wall and joints and as auditory organs in the antennae [4–6]. In the fly CNS, *ato* is important not for specification but for axonal arborization [7]. *Math1*, in contrast, is required for the specification of cells in both the CNS and the PNS [8–11]. Furthermore, *Math1* serves a role in the development of secretory lineage cells in the gut, a function that does not parallel any known to be served by *ato* [12]. We wondered whether *ato* and *Math1* might be more functionally homologous than they appear, so we expressed *Math1* in *ato* mutant flies and *ato* in *Math1* null mice. To our surprise, the two proteins are functionally interchangeable.

Results and Discussion

Previous work from our labs has shown that ubiquitous expression of *Math1* under the control of a heat-shock promoter can induce the formation of chordotonal organs (CHOs) in the absence of *ato* [10]. It remained to be determined whether *Math1* could specify ectopic CHOs de novo or convert precursor cells that had already been selected by other proneural proteins such as Scute. We used the GAL4-UAS system [13] to express *Math1* in *ato* mutant embryos under the control of the *ato* embryonic enhancer [7, 10, 14]. This approach permits control of *Math1* expression in ectodermal cells that normally become sensory organ precursors of CHOs in stage 10/11 embryos [5, 7, 14]. In wild-type flies, only three of the five sensory-organ precursors that give rise to lateral CHOs express *ato*; the other two CHOs are recruited from the surrounding ectodermal cells through activation of the epidermal growth factor (EGF) signaling pathway [15]. Expression of one copy of *Math1* restored three of the five lateral CHOs (our unpublished data); two copies of *Math1* resulted in the specification of five, and occasionally six, CHOs (Figures 1A–1C). The degree of *Math1* rescue is the same as that achieved by expressing *ato* in these mutant flies under the same driver (our unpublished data). *Math1* thus fully compensated for the loss of *ato* in the fly; it allowed both precursor cell selection and CHO specification. *Math1*, like *ato*, is able to activate EGF receptor signaling in the fly.

Math1 rescued the other known aspects, such as lack of photoreceptors, of the *ato* null phenotype as well. Figures 1E and 1F show the markers senseless and α-chaoptin in third-instar eye antennal disks of *ato* larva expressing MATH1 ([16, 17]; Figure 1). *Math1* also induced ectopic photoreceptors in wild-type flies (our unpublished data). In the fly CNS, *ato* is known to be important for axonal arborization of the dorsal-cluster (DC) neurons [7]. *Math1* overexpression induced the same axonal aborization in these two neuronal clusters as *ato* overexpression does (Figures 1H and 1I). Importantly, we found no evidence that *Math1* induces expression of the *ato*-related gene *amos* (our unpublished data), which suggests that *Math1* is directly regulating *ato* target genes.

To ascertain which functions of *Math1* can be carried out by *ato* in the mouse, we replaced the *Math1* coding region with *ato* by using the gene-targeting strategy shown in Figure 2A. We then used targeted embryonic-stem (ES) cells to generate chimeras and heterozygous animals. We generated trans-heterozygote animals carrying $Math1^{ato}$ and $Math1^{lacZ}$ (a null allele of *Math1* in which the coding region is replaced by β-galactosidase) by intercrossing the heterozygous animals [10]. Southern blot analysis showed that the *Math1* coding region was replaced by *atonal*'s coding region in these animals (Figures 2D and 2E), and Northern blot analysis confirmed the absence of *Math1* mRNA (Figure 2F).

Math1 null animals fail to initiate respiration and die very shortly after of birth [8], but $Math1^{ato/lacZ}$ animals carrying a single allele of *ato* survived to adulthood and appeared normal by observation and by histological analysis (our unpublished data). We therefore searched for subtle developmental abnormalities in tissues in which *Math1* is known to play an important role in cell differentiation by comparing $Math1^{ato/lacZ}$ and *Math1* null embryos.

At E18.5, the latest time-point at which they can be evaluated, *Math1* null mice lack two rhombic lip derivatives: the external granular layer (EGL), which contains the granule neuron precursors [8], and the pontine nucleus [10]. Both the EGL and pontine nuclei are normal in $Math1^{ato/lacZ}$ mice at this stage of development (Figure 3). We next examined the developing spinal cord. We have shown in previous work that *Math1* governs the

[6]Correspondence: hzoghbi@bcm.tmc.edu
[7]These authors contributed equally to this work.

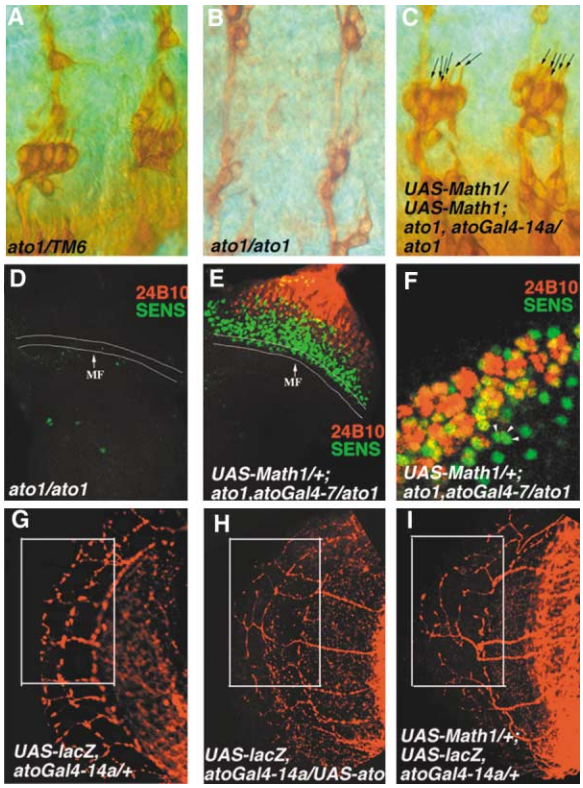

Figure 1. *Math1* Produces Chordotonal Organs, Photoreceptors, and Axonal Arborization in Stage 16 *ato* Mutant Embryos

(A) Lateral view of two abdominal segments of a heterozygous embryo, stained with neuronal marker 22C10, showing the five neurons of the lateral chordotonal cluster.

(B) Lateral view of *ato* mutant embryo lacking lateral chordotonal neurons.

(C) Lateral view of a 22C10-stained *ato* mutant embryo expressing two copies of *Math1* under the control of the embryonic *ato* enhancer element. The normal complement of five lateral chordotonal neurons is restored in one hemisegment (right), and an ectopic sixth neuron is generated in another (left).

(D) Third-instar larval eye-antennal disc from an *ato* mutant larva stained with the R8 marker α-Senseless (green) and the photoreceptor marker α-Chaoptin (24B10, red). Neither marker is detectable. MF marks the morphogenetic furrow.

(E) Third-instar larval eye-antennal disc from an *ato* mutant larva expressing MATH1 anterior to the MF under the Gal4-7 driver shows staining with α-Senseless (green) and α-Chaoptin (24B10, red). R8 photoreceptors are recovered. Since Gal4-7 does not mimic *ato* expression well, the organization of the rescued ommatidia is irregular.

(F) Third-instar larval eye-antennal disc from a larva overexpressing MATH1 in a wild-type background stained with α-Senseless (green) and α-Chaoptin (24B10, red). Overexpression of MATH1 produces ectopic R8 cells (arrowheads) and disrupts ommatidial organization.

(G) Adult brain from a control fly expressing β-Gal in DC neurons under the control of the *ato* enhancer. The panel shows the normal pattern of arborization in the distal medulla (boxed).

(H) Adult brain of the same genetic background as in (G) overexpressing *ato* and showing an abnormal arborization pattern in the distal medulla.

(I) Adult brain of the same genetic background as in (G) overexpressing *Math1* and showing an abnormal arborization pattern almost identical to that caused by *ato* overexpression.

development of the D1 interneurons [11]. The D1 interneuron precursors migrate ventrally from the dorsal spinal cord to settle in the deep dorsal horn, where they differentiate into neurons that give rise to some of the spinocerebellar tracts. In *Math1* null mice the D1 neurons fail to migrate; instead, they accumulate in the dorsal aspect of the spinal cord (Figure 3I). However, normal migration of these precursors can be seen in both $Math1^{lacZ/+}$ and $Math1^{ato/lacZ}$ mice (Figures 3G and 3H). Moreover, unlike the null animals [11], the D1 interneuron precursors in $Math1^{ato/lacZ}$ mice express several markers, such as Lh2A (our unpublished data).

Math1 is essential for the formation of inner-ear hair cells [9]. The inner-ear hair cells of the cochlea and balance organs (Figures 4A and 4B and data not shown) appear normal by histological criteria in the $Math1^{ato/lacZ}$ animals; there are three rows of outer hair cells and a single row of inner hair cells in the cochlea. These hair cells express appropriate differentiation markers such as calretinin (our unpublished data). To ascertain whether the $Math1^{ato/lacZ}$ mice might suffer functional deficits despite their apparently normal histology, we tested hearing in both $Math1^{ato/lacZ}$ and wild-type mice. In auditory brainstem response assays, the $Math1^{ato/lacZ}$ mice displayed a physiological response similar to that of control animals (our unpublished data), indicating that their hearing is not impaired. The hair cells are thus both histologically normal and functional in $Math1^{ato/lacZ}$ mice.

To uncover any subtle deficits in coordination, we tested the $Math1^{ato/lacZ}$ mice on the rotating-rod apparatus [18]. As shown in Figure 4D, there were no significant differences between the performances of $Math1^{ato/lacZ}$ mice and their wild-type littermates. These data strongly suggest that the balance pathways in the $Math1^{ato/lacZ}$ mice are not only histologically normal but fully functional as well.

Outside of the hearing and proprioceptive pathways, *ato* rescues the null phenotype associated with the loss of *Math1* in the developing gut. *Math1* is essential for the differentiation and development of the secretory-cell lineage (enteroendocrine cells, goblet cells, and Paneth cells) [12]. Normal gut development in $Math1^{ato/lacZ}$ mice was evidenced by expression of markers such as chromogranin A that are normally expressed in enteroendocrine cells (Figure 5). Goblet cells were morphologically normal as well (our unpublished data).

Lastly, we considered the possibility that *ato* could be acting indirectly in these mice through *Math5*, the closest homolog of *Math1*. There was no evidence of ectopic *Math5* activation (our unpublished data), suggesting that *ato* is acting directly on *Math1* target genes in these mice.

We conclude that *ato* and *Math1* are functionally interchangeable in flies and mice. Many vertebrate genes have been shown to be capable of substituting for the functions of their invertebrate counterparts [19–22], but only two invertebrate genes have been found thus far to restore any portion of the null phenotype in a mammal—and none produces a full functional recovery [1, 2].

It is striking that *ato* and *Math1* show such overlap in function despite their limited sequence similarity. There is only 68% identity in the 57 amino acid bHLH domain; the 12 amino acids that form the basic domain are identi-

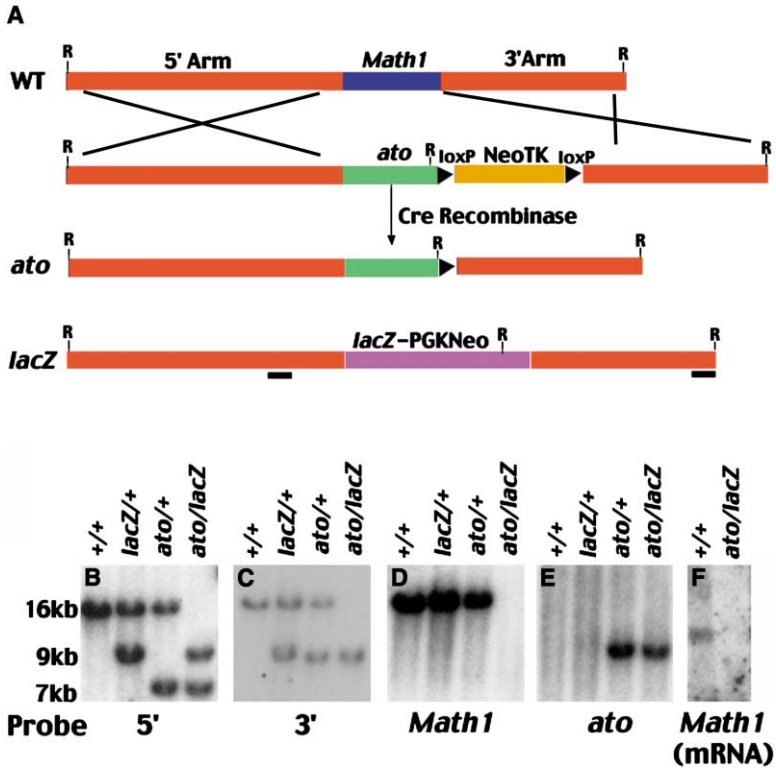

Figure 2. *Math1* Coding Region Replaced by *Drosophila ato*

(A) Diagram of knock-in strategy and final generation of *ato* knock-in allele. The bottom of the panel shows the *Math1* null allele that expresses *lacZ*. The locus is not drawn to scale; R = EcoRI, and black squares denote the position of the 5′ and 3′ probes.

(B and C) Southern blots of tail DNA; the 5′ (B) and 3′ (C) probes were used. In (B), the 16 kb band represents the wild-type allele, the 9 kb band represents the $Math1^{lacZ}$ allele, and the 7 kb band represents the $Math1^{ato}$ allele. In (C), the 16 kb band represents the wild-type allele, while the 9 kb band represents the $Math1^{lacZ}$ and $Math1^{ato}$ alleles.

(D) Southern blot of tail DNA; the *Math1* coding region was used as a probe. The blot shows the deletion of the coding region in the $Math1^{ato/lacZ}$ mice.

(E) Southern blot of tail DNA; the *ato* coding region was used as a probe. The *ato* coding sequence is clearly present in the $Math1^{ato/lacZ}$ mice.

(F) Northern blot probed with the bHLH coding region of *Math1*. There is no *Math1* mRNA in a $Math1^{ato/lacZ}$ E12.5 embryo.

cal between *ato* and *Math1*. There is no similarity, however, between the approximately 300 remaining amino acids of the two proteins [23, 24]. Although we cannot exclude the possibility that there might be conserved protein structures, it appears that *Math1*'s "new" functions in the mouse (gut) seem to arise from expression in a new environment rather than the acquisition of a new domain. Changes in *cis*-regulatory elements have been proposed to cause differences in gene expression, an important driving force of evolution. Several years ago, Xue and Noll proposed that genes may acquire new regulatory elements, and eventually new functions,

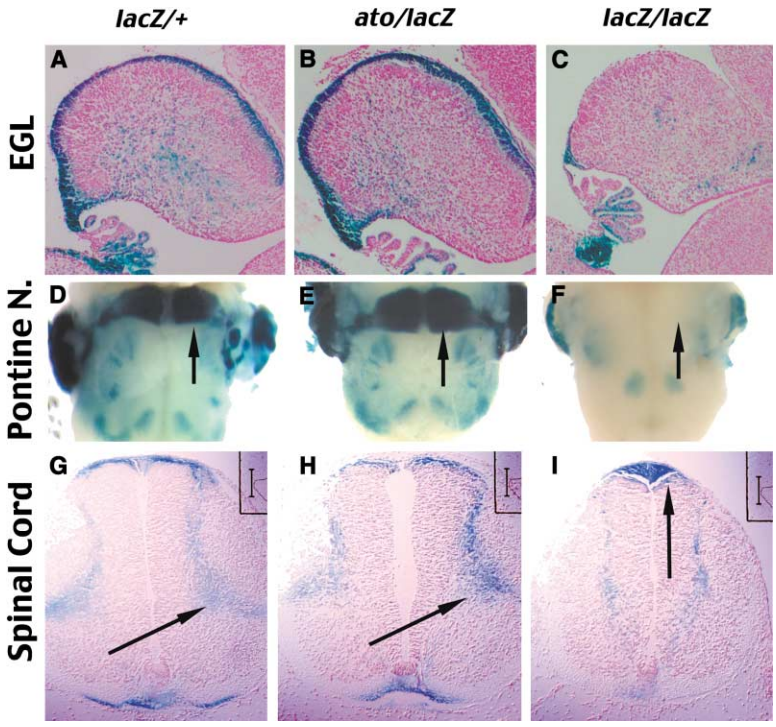

Figure 3. Normal CNS Development in $Math1^{ato/lacZ}$ Mice

At E18.5, the $Math1^{lacZ}$ allele drives β-galactosidase expression in the EGL and pontine nuclei. $Math1^{lacZ/+}$ (A) and $Math1^{ato/lacZ}$ (B) mice have a normal external granule layer (EGL), whereas $Math1^{lacZ/lacZ}$ (C) mice lack an EGL. (D–F) Views of the ventral area of the brainstem showing the pontine nucleus (arrow) in $Math1^{lacZ/+}$ (D) and $Math1^{ato/lacZ}$ (E) mice but not in $Math1^{lacZ/lacZ}$ animals (F). (G–I) A section of the cervical spinal cord from an E12.5 embryo. The D1 interneurons (marked by the β-galactosidase reporter gene) have migrated to the deep dorsal horn (arrow) in $Math1^{lacZ/+}$ (G) and $Math1^{ato/lacZ}$ (H) mice. (I) In the $Math1^{lacZ/lacZ}$ mice, the cells that should give rise to D1 interneurons do not migrate and remain in the dorsal aspect of the spinal cord (arrow).

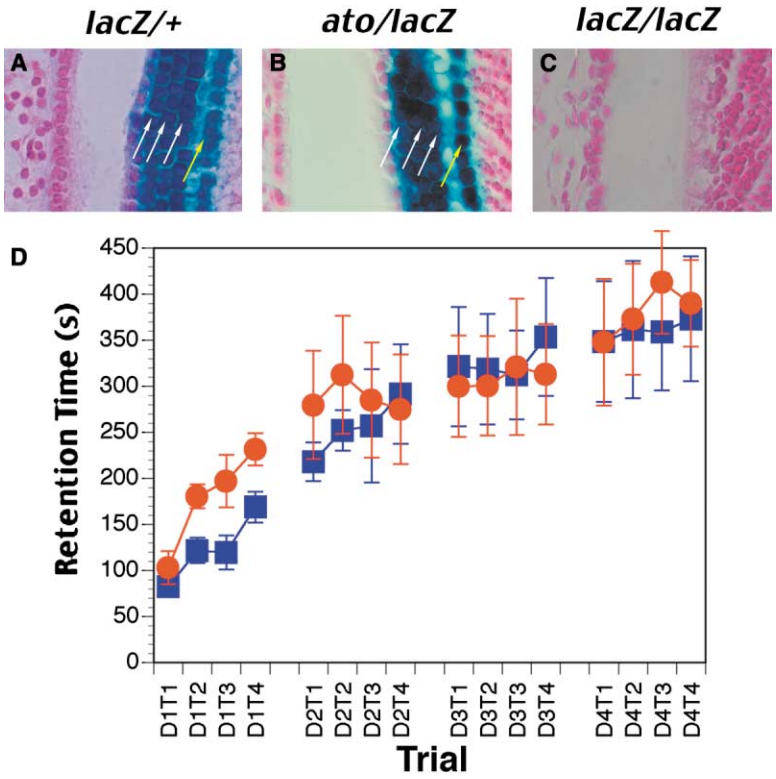

Figure 4. Inner-Ear Hair Cell Development and Coordination Are Normal in *Math1*$^{ato/lacZ}$ Mice

(A–C) At E18.5, the three rows of outer-ear hair cells (white arrows) and one row of inner hair cells (yellow arrow) express β-galactosidase in *Math1*$^{lacZ/+}$ (A) and *Math1*$^{ato/lacZ}$ (B) mice. The outer and inner rows of hair cells are absent in the *Math1*$^{lacZ/lacZ}$ mice (C).

(D) Analysis of results of rotating-rod test. *Math1*$^{ato/lacZ}$ mice (red) do not display motor learning, balance, or coordination defects and perform similarly to their wild-type littermates (blue). N = 7 for each genotype.

as a result of gene duplication events [25]. This hypothesis is substantiated by a large body of work showing that many proteins can function in place of their paralogs, e.g., *Hox* genes can substitute for each other in patterning the axial skeleton [26–28]. Similarly, studies in both *Drosophila* and mice have shown that several *Pax* genes can rescue portions of the null phenotype of another *Pax* family member [25, 29, 30]. Gene duplication events are not strictly necessary, however [31]; studies in crustaceans suggest that changes in homeotic gene expression may be sufficient to explain differences in appendages [32, 33].

Although these paralogous genes can largely substitute for each other, they are not equivalent [27, 30]—with the exception of *Hoxa3* and *Hoxd3* [26]. This suggests that certain new functions result from changes in coding sequence. Comparisons of orthologous genes have identified gene-specific and species-specific domains such as the ones in *Ubx* that are responsible for differences in body patterning in insects [34, 35].

We are unaware of another pair of orthologs besides *ato* and *Math1* that show full functional conservation between mouse and *Drosophila*. Our data argue that *Math1*'s new functions in the mouse were acquired through the evolution of *cis*-regulatory factors that result in its expression in new tissues. Interestingly, the two *ato* homologs in mice, *Math1* and *Math5,* together recapitulate the expression pattern of *ato* in *Drosophila*. Further studies are necessary to determine whether these two paralogs are functionally equivalent as well.

Experimental Procedures

Fly Strains and Immunohistochemistry

ato Gal4-14A and UAS-*Math1* strains are as described [7, 10]. All flies were raised on standard fly food at 25°C, and targeted expression crosses were set at 28°C. Immunohistochemistry was performed as previously described [7]. In short, embryos, imaginal discs, and adult brains were fixed, blocked in 1× PAXDG (1× PBS with 1% BSA, 0.3% Triton-X, 0.3% sodium deoxycholate, and 5% normal goat serum) for 1 hr at room temperature and incubated with the appropriate dilutions of antibodies (22C10, 1:100; 24B10, 1:200; mouse α-βGal, Promega, 1:3000; α-SENS, 1:1000; α-AMOS, 1:1000) in PAXDG at 4°C overnight, followed by a 1 hr wash in PXDG (1× PBS with 0.3% Triton-X, 0.3% sodium deoxycholate, and 5% normal

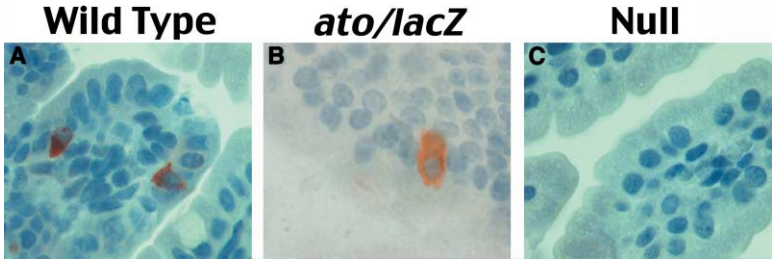

Figure 5. Enteroendocrine Cell Development Is Normal in *Math1*$^{ato/lacZ}$ Mice

Enteroendocrine cells, marked by the staining of chromogranin A (brown cells), are present in wild-type (A) and *Math1*$^{ato/lacZ}$ (B) mice but not in *Math1* null mice (C).

goat serum) and a 10 min wash in 1× PBT. Stained embryos were mounted in 70% glycerol in 1× PBS.

Generation of the *Math1^{ato}* Allele

The *atonal* open reading frame was amplified by PCR from a plasmid containing *ato* cDNA. Upon sequencing, it was ligated with the 5′ arm, the 3′ arm and the Neo-TK selectable cassette (containing the neomysin phosphotransferase gene under the control of the PGK promoter and the thymidine kinase gene under the HSV1 promoter) to generate the targeting vector.

Generation and selection of ES cell clones and generation of chimera were as previously described [36]. In brief, ES cells were electroporated with the targeting vector and selected for G418 resistance. Resistant clones were checked for recombination at the *Math1* locus. A plasmid expressing CRE recombinase was then electroporated into the clones to remove the selectable cassette under FIAU selection. Clones without the selectable cassette were then used for blastocyst injection. The *lacZ* allele used in this experiment is a null allele of *Math1* with the coding region replaced by the *lacZ* gene.

β-Galactosidase Staining, Immunofluorescence, and Immunohistochemistry

In brief, and as described previously [9, 10], embryos were dissected in phosphate-buffered saline (PBS), fixed in 4% paraformaldehyde (PFA) solution for 20–30 min, washed thoroughly in PBS, and equilibrated in X-gal staining buffer (5 mM potassium ferricyanide, 5 mM potassium ferrocyanide, 0.02% NP40, and 0.01% sodium deoxycholate). Embryos were stained overnight in X-gal buffer with X-gal (1 mg/ml), then post-fixed in 4% PFA, dehydrated, embedded, and sectioned with a microtome. Sections were counter-stained with nuclear fast red. Immunofluorescence (calretinin, from Chemicon; dilution 1:200) and immunohistochemistry (22C10, at dilution 1:100; Lh2A/B from T. Jessell, used at 1:1000 dilution; Chromogranin A, DiaSorin, 1:1000) were performed as previously described [7, 9–11].

Rotarod Analysis

We placed eight-week-old mice on the rotating-rod apparatus, which accelerates from 4 rpm to 40 rpm over a 4.5 min period, and recorded how long the mice stayed on the rod [36]. Four trials were done per day, four days in a row, with a 20 min break between trials.

Auditory Brainstem Response

We tested the ABR by placing electrodes on anesthetized mice at the vertex and behind the ear; responses to 5 ms-long pulses were recorded and averaged [37].

Acknowledgments

We thank W. Brownell and C. Shope for the auditory brainstem response assays; T. Jessell for Lh2A/B antibody and A. Jarman for sharing the AMOS antibody before publication; B. Antalffy and B. Xu for technical assistance; G. Halder for useful comments on the manuscript; and K. Schulze and V. Brandt for editorial advice. H.J.B. and H.Y.Z. are investigators of the Howard Hughes Medical Institute. B.A.H. and V.Y.W. were supported by a postdoctoral and a predoctoral National Research Service Award, respectively. V.Y.W. is a McNair fellow. B.A.H. is a Flanders Interuniversity Institute of Biotechnology group leader. This research is supported by a National Aeronautics and Space Administration grant to H.J.B. and H.Y.Z.

Received: April 18, 2002
Revised: June 24, 2002
Accepted: July 17, 2002
Published: September 17, 2002

References

1. Acampora, D., Avantaggiato, V., Tuorto, F., Barone, P., Reichert, H., Finkelstein, R., and Simeone, A. (1998). Murine Otx1 and Drosophila otd genes share conserved genetic functions required in invertebrate and vertebrate brain development. Development *125*, 1691–1702.
2. Hanks, M.C., Loomis, C.A., Harris, E., Tong, C., Anson-Cartwright, L., Auerbach, A., and Joyner, A. (1998). Drosophila engrailed can substitute for mouse Engrailed1 function in mid-hindbrain, but not limb development. Development *125*, 4521–4530.
3. Grenier, J.K., and Carroll, S.B. (2000). Functional evolution of the Ultrabithorax protein. Proc. Natl. Acad. Sci. USA *97*, 704–709.
4. Jarman, A.P., Grau, Y., Jan, L.Y., and Jan, Y.N. (1993). atonal is a proneural gene that directs chordotonal organ formation in the Drosophila peripheral nervous system. Cell *73*, 1307–1321.
5. Jarman, A.P., Sun, Y., Jan, L.Y., and Jan, Y.N. (1995). Role of the proneural gene, atonal, in formation of Drosophila chordotonal organs and photoreceptors. Development *121*, 2019–2030.
6. Eberl, D.F. (1999). Feeling the vibes: chordotonal mechanisms in insect hearing. Curr. Opin. Neurobiol. *9*, 389–393.
7. Hassan, B.A., Bermingham, N.A., He, Y., Sun, Y., Jan, Y.N., Zoghbi, H.Y., and Bellen, H.J. (2000). *atonal* regulates neurite arborization but does not act as a proneural gene in the *Drosophila* brain. Neuron *25*, 549–561.
8. Ben-Arie, N., Bellen, H.J., Armstrong, D.L., McCall, A.E., Gordadze, P.R., Guo, Q., Matzuk, M.M., and Zoghbi, H.Y. (1997). Math1 is essential for genesis of cerebellar granule neurons. Nature *390*, 169–172.
9. Bermingham, N.A., Hassan, B.A., Price, S.D., Vollrath, M.A., Ben-Arie, N., Eatock, R.A., Bellen, H.J., Lysakowski, A., and Zoghbi, H.Y. (1999). Math1: an essential gene for the generation of inner ear hair cells. Science *284*, 1837–1841.
10. Ben-Arie, N., Hassan, B.A., Bermingham, N.A., Malicki, D.M., Armstrong, D., Matzuk, M., Bellen, H.J., and Zoghbi, H.Y. (2000). Functional conservation of atonal and Math1 in the CNS and PNS. Development *127*, 1039–1048.
11. Bermingham, N.A., Hassan, B.A., Wang, V.Y., Fernandez, M., Banfi, S., Bellen, H.J., Fritzsch, B., and Zoghbi, H.Y. (2001). Proprioceptor pathway development is dependent on Math1. Neuron *30*, 411–422.
12. Yang, Q., Bermingham, N.A., Finegold, M.J., and Zoghbi, H.Y. (2001). Requirement of Math1 for secretory cell lineage commitment in the mouse intestine. Science *2294*, 2155–2158.
13. Brand, A.H., and Perrimon, N. (1993). Targeted gene expression as a means of altering cell fates and generating dominant phenotypes. Development *118*, 401–415.
14. Sun, Y., Jan, L.Y., and Jan, Y.N. (1998). Transcriptional regulation of atonal during development of the Drosophila peripheral nervous system. Development *125*, 3731–3740.
15. Okabe, M., and Okano, H. (1997). Two-step induction of chordotonal organ precursors in Drosophila embryogenesis. Development *124*, 1045–1053.
16. Frankfort, B.J., Nolo, R., Zhang, Z., Bellen, H., and Mardon, G. (2001). *senseless* repression of *rough* is required for R8 photoreceptor differentiation in the developing *Drosophila* eye. Neuron *32*, 403–414.
17. Reinke, R., Krantz, D.E., Yen, D., and Zipursky, S.L. (1988). Chaoptin, a cell surface glycoprotein required for *Drosophila* photoreceptor cell morphogenesis, contains a repeat motif found in yeast and human. Cell *52*, 291–301.
18. Voikar, V., Koks, S., Vasar, E., and Rauvala, H. (2001). Strain and gender differences in the behavior of mouse lines commonly used in transgenic studies. Physiol. Behav. *72*, 271–281.
19. McGinnis, N., Kuziora, M.A., and McGinnis, W. (1990). Human Hox-4.2 and *Drosophila* Deformed encode similar regulatory specificities in *Drosophila* embryos and larvae. Cell *63*, 969–976.
20. Malicki, J., Schughart, K., and McGinnis, W. (1990). Mouse Hox-2.2 specifies thoracic segmental identity in *Drosophila* embryos and larvae. Cell *63*, 961–967.
21. Zhang, J.M., Chen, L., Krause, M., Fire, A., and Paterson, B.M. (1999). Evolutionary conservation of MyoD function and differential utilization of E proteins. Dev. Biol. *208*, 465–472.
22. Rincon-Limas, D.E., Lu, C.H., Canal, I., Calleja, M., Rodriguez-Esteban, C., Izpisua-Belmonte, J.C., and Botas, J. (1999). Conservation of the expression and function of apterous orthologs in Drosophila and mammals. Proc. Natl. Acad. Sci. USA *96*, 2165–2170.
23. Akazawa, C., Ishibashi, M., Shimizu, C., Nakanishi, S., and Kageyama, R. (1995). A mammalian helix-loop-helix factor struc-

turally related to the product of Drosophila proneural gene atonal is a positive transcriptional regulator expressed in the developing nervous system. J. Biol. Chem. *270*, 8730–8738.
24. Ben-Arie, N., McCall, A.E., Berkman, S., Eichele, G., Bellen, H.J., and Zoghbi, H.Y. (1996). Evolutionary conservation of sequence and expression of the bHLH protein atonal suggests a conserved role in neurogenesis. Hum. Mol. Genet. *5*, 1207–1216.
25. Xue, L., and Noll, M. (1996). The functional conservation of proteins in evolutionary alleles and the dominant role of enhancers in evolution. EMBO J. *15*, 3722–3731.
26. Greer, J.M., Puetz, J., Thomas, K.R., and Capecchi, M.R. (2000). Maintenance of functional equivalence during paralogous Hox gene evolution. Nature *403*, 661–665.
27. Zhao, Y., and Potter, S.S. (2002). Functional comparison of the Hoxa *4*, Hoxa *10*, and Hoxa 11 homeoboxes. Dev. Biol. *244*, 21–36.
28. Zakany, J., Gerard, M., Favier, B., Potter, S.S., and Duboule, D. (1996). Functional equivalence and rescue among group 11 Hox gene products in vertebral patterning. Dev. Biol. *176*, 325–328.
29. Bouchard, M., Pfeffer, P., and Busslinger, M. (2000). Functional equivalence of the transcription factors Pax2 and Pax5 in mouse development. Development *127*, 3703–3713.
30. Xue, L., Li, X., and Noll, M. (2001). Multiple protein functions of paired in Drosophila development and their conservation in the Gooseberry and Pax3 homologs. Development *128*, 395–405.
31. Carroll, S.B. (1995). Homeotic genes and the evolution of arthropods and chordates. Nature *376*, 479–485.
32. Abzhanov, A., and Kaufman, T.C. (1999). Novel regulation of the homeotic gene Scr associated with a crustacean leg-to-maxilliped appendage transformation. Development *126*, 1121–1128.
33. Averof, M., and Patel, N.H. (1997). Crustacean appendage evolution associated with changes in Hox gene expression. Nature *388*, 682–686.
34. Ronshaugen, M., McGinnis, N., and McGinnis, W. (2002). Hox protein mutation and macroevolution of the insect body plan. Nature *415*, 914–917.
35. Galant, R., and Carroll, S.B. (2002). Evolution of a transcriptional repression domain in an insect Hox protein. Nature *415*, 910–913.
36. Matilla, A., Roberson, E.D., Banfi, S., Morales, J., Armstrong, D.L., Burright, E.N., Orr, H.T., Sweatt, J.D., and Zoghbi, H.Y. (1998). Mice lacking ataxin-1 display learning deficits and decreased hippocampal paired-pulse facilitation. J. Neurosci. *18*, 5508–5516.
37. Liu, M., Pereira, F.A., Price, S.D., Chu, M.J., Shope, C., Himes, D., Eatock, R.A., Bronwnell, W.E., and Lysakowski, A. (2000). Essential role of BETA2/NeuroD1 in development of the vestibular and auditory systems. Genes Dev. *14*, 2839–2854.